

Article

Sorption–Dilatometric Properties of Coal from a High-Methane Mine in a CO₂ and CH₄ Atmosphere

Paweł Baran ^{1,*} , Stanisław Kozioł ¹, Katarzyna Czerw ¹, Adam Smoliński ² and Katarzyna Zarębska ¹

¹ Faculty of Energy and Fuels, AGH University of Science and Technology, Al. Mickiewicza 30, 30-059 Cracow, Poland

² Department of Energy Saving and Air Protection, Central Mining Institute, Pl. Gwarków 1, 40-166 Katowice, Poland

* Correspondence: baranp@agh.edu.pl; Tel.: +48-12-617-20-79

Abstract: Although highly developed countries are trying to diversify away from coal-based energy, many economies rely on this resource. Its consumption results in the production of carbon dioxide, which promotes global warming, necessitating its sequestration. This paper presents the sorption–dilatometric relationships of hard coal samples differing in vitrinite and inertinite content. The studies were carried out under isothermal conditions (298 K) at a free pressure drop complemented by measurements under non-isothermal conditions (298 K to 323 K). The tests were performed on an original apparatus, based on the operation of an Arduino microcontroller. For the natural porosity to be preserved and for a better representation of the behaviour of the coal–gas system, samples in the form of cuboidal blocks were used, making this apparatus unique worldwide. Based on the study, it appears that the difference in petrographic composition affects the behaviour of the coal structure, influencing differences in the sorption–dilatometric properties. In the case of the sample with higher vitrinite content, the amount of adsorbed gases is higher.

Keywords: coal; methane; carbon dioxide; sorption; swelling



Citation: Baran, P.; Kozioł, S.; Czerw, K.; Smoliński, A.; Zarębska, K.

Sorption–Dilatometric Properties of Coal from a High-Methane Mine in a CO₂ and CH₄ Atmosphere. *Energies* **2023**, *16*, 1785. <https://doi.org/10.3390/en16041785>

Academic Editor: Krzysztof Skrzypkowski

Received: 28 December 2022

Revised: 4 February 2023

Accepted: 8 February 2023

Published: 10 February 2023



Copyright: © 2023 by the authors. Licensee MDPI, Basel, Switzerland. This article is an open access article distributed under the terms and conditions of the Creative Commons Attribution (CC BY) license (<https://creativecommons.org/licenses/by/4.0/>).

1. Introduction

Despite the transition away from fossil fuels, hard coal is still in the top three fuels in the world's energy industry [1,2]. With increasing urbanization and population, the demand for coal is still high. As a result, there is a continuous increase in anthropogenic carbon dioxide emission, which is one of the causes of global warming. Therefore, measures are being taken to reduce emissions of this gas, with particular emphasis on point source emitters [3]. In addition, 195 countries have accepted the so-called Paris Agreement. By doing so, they have committed to reducing greenhouse gas emissions, with a 2 °C reduction in temperature relative to the pre-industrial era as one of the main goals. In addition, more than 20 countries around the world have pledged to achieve a mission of net-zero emissions by investing in renewable energy and other technologies with reduced carbon dioxide emissions [4,5]. In terms of the method of carbon dioxide capture, post-combustion technology, pre-combustion technology, and oxygen combustion technology can be distinguished [6]. One method is geological sequestration [7]. Underground sites with storage potential include oil fields, gas fields, and subeconomic coal seams. In this case, 65 commercial CCS facilities are operating worldwide [8]. Among them, 26 are operating, 13 are in an advanced stage of development reaching front-end engineering design, 21 installations are at very early development stages, and 2 have suspended operations (mainly due to the economic downturn). In 2020, worldwide commercial facilities captured and stored ~40 Mt CO₂ per year.

Due to the global tendency to increase the diversification of energy sources, coalbed methane (CBM) has become an area of scientific interest. Its greatest advantages include its calorific value and its high quality as an energy carrier [9]. An additional advantage

is the use of this gas as an input product in the production of hydrogen, which is often referred to as the fuel of the future. Apart from natural geological traps, which prevent methane from reaching the surface, methane is stored in coal beds inside the coal matrix due to the adsorption mechanism. To extract methane trapped in geological traps, the permeability of rock formations must be altered. The most common solution is the process of hydraulic fracturing. This process involves injecting a fracturing fluid, consisting of water, sand, and other chemical additives into a wellbore. As a result, natural fractures within the gas-bearing horizon are widened and new ones are created, allowing gas to escape through gaps in the bed [10]. To release the methane adsorbed inside the coal matrix, a series of physicochemical processes must be used. Hard coal, as a naturally porous material, has a system of micro- and macropores inside its structure, forming a biporous system [11]. Bituminous coal is composed of organic matter mixed with inorganic matter, and its elemental and petrographic composition may vary significantly. For this reason, understanding the process of methane adsorption on hard coal has a significant impact on subsequent attempts to extract methane gas from subeconomic hard coal seams. Some studies have suggested that the sorption capacity of coals is influenced by parameters such as the degree of coalification, the content of maceral moisture, rank and mineral content, and elemental composition [12–16]. When analysing the differences in methane and carbon dioxide adsorption on carbon of different origins, the most important parameter is the vitrinite reflectance (R_0). As R_0 increases, the sorption capacity towards CO_2 increases [17]. Jian et al. have shown in analyses of hard coal samples with high R_0 that changes in sorption capacity towards CO_2 are very small. Conversely, as the R_0 value decreases, changes in the sorption capacity of coal towards methane increase. Differences in the sorption capacity of hard coal towards CH_4 are also related to the maceral composition. Research has proven that coal with high content of vitrinite is characterised by higher sorption capacity than coal with higher content of inertinite [18,19]). The reason for such behaviour is a difference in the structure of particular macerals. Vitrinite shows a predominance of micropores, which therefore have the highest total volume, inertinite shows a predominance of mesopores, and liptinite is the least porous maceral [20]. Laxminarayana and co-workers [21] analysed coal samples from Australian mines, differing in the content of individual macerals. Vitrinite-rich coals were characterised by a fast methane desorption process. Coals with high inertinite content were characterised by slower sorption. Moreover, with increasing rank for inertinite-rich coals, the diffusion rate decreased. Similar observations occurred when vitrinite-rich coals were examined. In this case, the changes were not as pronounced. However, the trend was similar. When analysing the changes in the structure of hard coals accompanying increases in rank, one can observe a decrease in the number of meso- and macropores, which translates directly into a decrease in the rate of methane diffusion in the coal matrix [21–23].

By combining the process of geological sequestration of carbon dioxide with the process of extraction of methane adsorbed in the coal matrix, the ECBM process was developed [24]. It exploits the phenomenon of preferential sorption and pore occupation in the coal structure by carbon dioxide relative to methane, promoting the simultaneous desorption of methane to enable its extraction. Thus, this process is an alternative to traditional methane extraction and allows for the geological sequestration of large amounts of CO_2 in off-balance coal seams [25]. Laboratory studies conducted on cuboidal samples of hard coal show that for coals of similar rank, the sorption kinetics of methane and carbon dioxide have a similar relative rate, while the sorption capacity of CO_2 is twice as high as for methane [26]. One of the reasons for this behaviour may be the difference in molecule diameter. Carbon dioxide is characterised by a linear and centrosymmetric molecule with sp -hybridisation of central atom. Methane, on the other hand, is characterised by a tetrahedral structure with sp^3 hybridisation, which makes it occupy more space than CO_2 . Additionally, there is an observable difference between the diameters of the two molecules. Methane has a kinetic diameter of 380 pm, while carbon dioxide has a kinetic diameter of 330 pm. Therefore, some pores with small diameters inside the coal matrix can be

preferentially occupied by carbon dioxide molecules. A second reason for the preferential sorption of CO₂ is the characteristic interaction of this gas with the coal matrix, which allows the gas to dissolve inside the matrix [27].

The process of sorption of carbon dioxide and methane on hard coal is linked with the process of swelling/shrinking of the coal matrix. This phenomenon can cause the coal to crack, changes the durability, and thus releases stored CO₂. Research carried out on samples in the form of solid, cuboid blocks [28] as well as cylindrical samples [29] has shown that as the number of adsorbed vapours and gases increases, the linear dimensions of the samples change for both methane and carbon dioxide. The magnitude of deformation, however, varies depending on the elemental and maceral composition of hard coal. Hard coal, characterised by a higher vitrinite content, undergoes greater deformation than samples with a higher inertinite content. The cited publications focused mainly on the study of the effect of gases such as methane or carbon dioxide on the behaviour of coal material, with an emphasis on the elemental composition of coal. It should be remembered, however, that the content of individual macerals may vary significantly despite a very similar elemental composition.

When analysing the physical basis of the sorption process, the influence of temperature must be borne in mind. The coal bed is exposed to certain temperature fluctuations, which translate into changes in the behaviour of the coal–gas system. For this reason, performing studies on the sorption of vapours and gases under isothermal conditions is insufficient, and it is necessary to carry out studies under changing temperature conditions. As the temperature increases, some of the vapours and gases may be desorbed [30], which may pose certain risks in the process of the geological storage of carbon dioxide. Some studies have shown that the opposite is true. As the temperature increases by 1 K, a 2% increase in the rate of sorption kinetics is observed (e.g., Wang et al. [31]). Due to the lack of data in the literature, this article discusses the sorption-induced swelling properties of hard coal in a methane and carbon dioxide atmosphere.

The vast majority of mines in the Upper Silesian Coal Basin are mined under conditions of high methane concentration [32]. Due to the fact that Polish hard coal is usually mined from a depth of 700–1000 m, the seams characterized by one of the highest methane-bearing capacities are mined. The coal used for the research described in this article comes from one of the most methane-affected mines [33]. It produces high-quality coking coal, a critical raw material, and the company that owns the mine is the largest producer in the European Union. Over the past 20 years, in Polish mines, there have been three significant disasters related to methane outbursts at the mine. In the first, during the tunnelling of a pipe lunette at the level of 1000 m, an additional methane and rock outburst occurred after setting off explosive charges. The concentration of methane was 84% at the face of the wall. Shortly after this disaster, another incident occurred. During the ventilation of one of the pit walls, the methane in the goaf ignited and then exploded. As a result, methane and burning gases ended up in the working space of the longwall [34]. The last catastrophe took place in April 2022. There was a series of three explosions that killed nine miners and rescuers, and seven people were trapped at a depth of 1000 m.

The studies were carried out on samples of similar elemental composition but different petrographic composition, where the main difference was the vitrinite-to-inertinite ratio. In the first part, the properties of hard coal were studied under isothermal conditions, with a free pressure drop caused by sorption processes. The second part of the experiment was carried out under non-isothermal conditions, where the temperature change was 25 °C.

2. Materials and Methods

Coal samples from the Upper Silesian Coal Basin were used. Both samples were obtained from the same coal mine. However, they came from two different seams that differed in depth. This is important because the potential CBM seams are not homogeneous and differ in their properties throughout their occurrence and depth. The elemental and

petrographic composition are presented in Table 1. The ultimate and proximate analysis was performed in the Central Mining Institute in Katowice.

Table 1. Specification of the tested coal samples.

Sample	C ^{daf} (%)	S ^{daf} (%)	H ^{daf} (%)	N ^{daf} (%)	O ^{daf} (%)	W ^a (%)	A ^a (%)	V ^{daf} (%)	Vitrinite (%)	Liptinite (%)	Inertinite (%)
P1	84.24	0.39	4.58	1.52	4.58	1.75	3.01	27.12	73	7	20
P2	84.96	0.58	4.60	1.70	3.76	0.68	3.78	25.50	53	8	39

The elemental analysis was performed in the Central Mining Institute in Katowice. The moisture content was determined in accordance with the procedure set forth in the standard PN-80/G-04511, while ash content was established in accordance with PN-80/G-04512. The oxygen content was computed as the remainder of 100%, taking into account the moisture and ash content. W: moisture content, A: ash content, V: volatile matter content, C, H, N, O, S: content of element C, H, N, O, S, respectively, a: analytical basis, daf: dry-ash-free basis.

As shown in Table 1, the main difference between the two samples is the result of the petrographic analysis, specifically vitrinite and inertinite content. A strength of the conducted research is the use of solid hard coal samples in the shape of rectangular blocks. Studies in the literature on sorption phenomena of hard coal describe tests on samples in powder and grain form. The use of cuboidal coal blocks preserves the natural porosity and enables strain measurements to be performed. To show the hard coal samples studied under magnification, SEM images are shown in Figures 1 and 2. They show differences in grain size and external surface texture. The apparatus used in the study has been constructed for this experiment so that sorption and dilatometric changes can be measured simultaneously. It is possible to record changes in the linear dimensions of a sample in a given time interval. This type of measurement is based on changes in the resistance of strain gauges placed perpendicularly and parallel to the layering of the coal sample. In the first stage of the experiment, sorption capacity, together with linear deformations, was measured under isothermal conditions at a temperature of 298 K. In the second part of the experiment, a manostat was introduced into the system. The modification of the measuring system made it possible to determine the dilatometric changes of the sample under constant pressure. The temperature at which the measurement was carried out was in the range of 298–323 K.

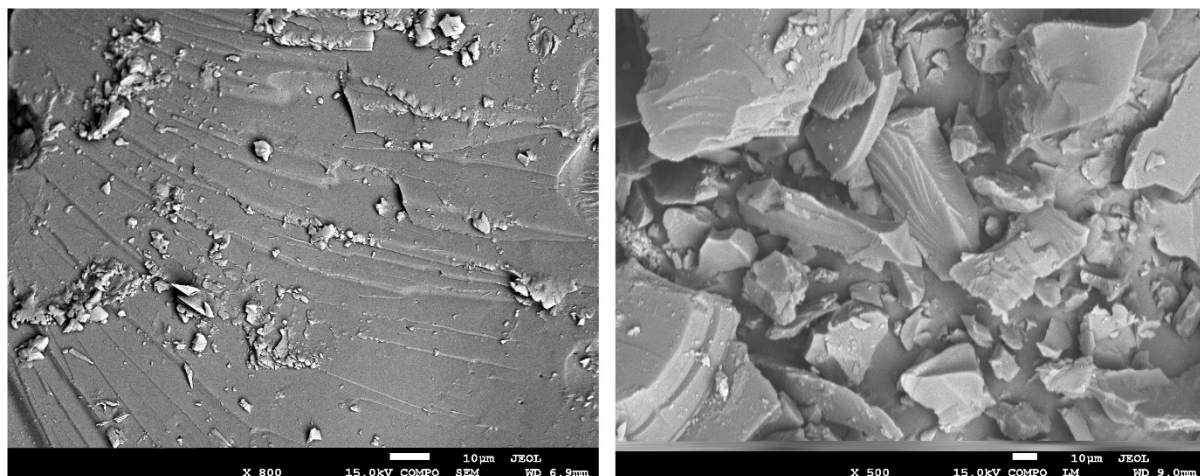


Figure 1. SEM images of the surface of sample P1.

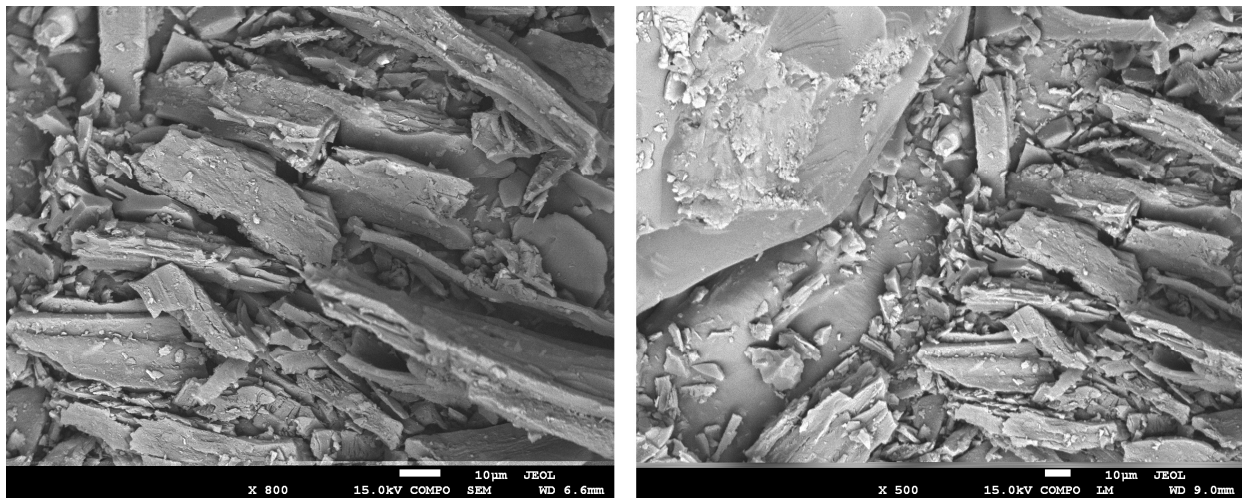


Figure 2. SEM images of the surface of sample P2.

3. Test Procedure

The measurements were made on a unique apparatus based on an Arduino microcontroller, which allows multiple parameters such as strain, pressure changes, and temperature measurements to be recorded simultaneously. It was built by the authors at the AGH University of Science and Technology in Kraków, Poland, and the proposed construction makes it adaptable to modifications and further improvements. In addition, a very wide library of software and the number of additional sensors allow the apparatus to be precisely adapted to the needs of the experiment performed. The implementation of the author's apparatus, combined with the hard coal samples subjected to analysis in the form of cuboidal solid blocks of coal, which is also not often found in the literature, makes the research performed unique. The wires coming out of the measuring ampoule were connected to a microcontroller. Tensometers were placed in the circuit based on the principle of a Wheatstone bridge. The experiment used resistance strain gauges with a resistance of $120 \pm 0.2\% \Omega$ and a strain sensitivity factor of $k = 2.1$. The tolerance of the k factor was 0.5%. From it, the signal is passed to a signal amplifier, based on the HX711 module, where the signal was converted to digital. Furthermore, the signal was sent to the Arduino UNO microcontroller. The results were recorded using the SD card reader module, and the current result is shown on the LCD1602 2×16 display with an I2C module. The pressure was measured using voltage S-20 transducers, which were operated in front of an additional Arduino UNO board with an LCD display. The schematic design of the device is shown in Figure 3, which includes the most important components of the device.

Cuboidal specimens were cut from the bulks of the bedrock. The linear dimensions of the samples were base 18×18 mm, walls 18×40 mm. The compensation sample had similar linear dimensions but was made of granite, a non-porous material. The weight of the samples used was approximately 20 g. Before the actual measurement, the samples were degassed with a vacuum pump. The vacuum value was 10^{-5} Pa, and the duration of degassing was 8 h. In addition, helium at a pressure of 10 kPa was passed through the sample to remove adsorbed vapours and gases inside the porous structure. The first point of the experiment was the introduction of the test gases into the ampoules with samples P1 and P2 and the compensation sample. In the second part of the experiment, the initial pressure was defined as the final pressure from the first part of the experiment. Next, the gas was introduced into the manostat and then into the measuring apparatus. Through the use of an electronic controller, the pressure in the apparatus was kept constant by gradually dosing the sorbate. The measurement temperature for the isothermal process was 298 K. Measurements under non-isothermal conditions, were conducted over the full temperature range of 298 K to 323 K.

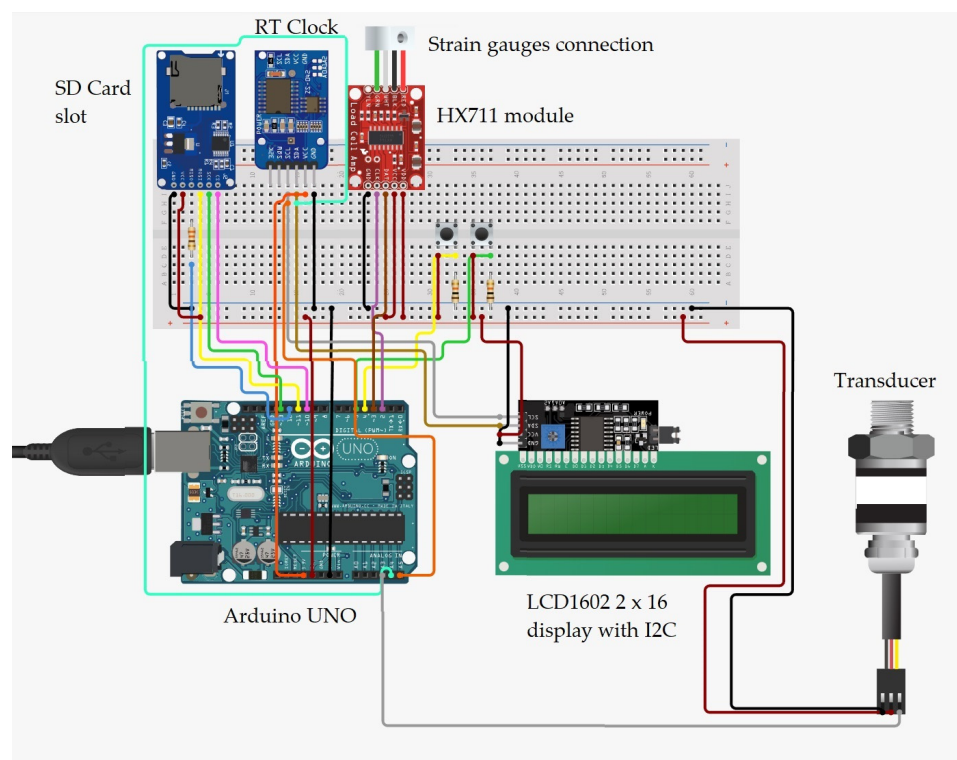


Figure 3. Schematic of the measurement system.

4. Results and Discussion

The sorption–dilatation results, for both samples, are presented in Figure 4a,b in the form of sorption kinetics. Both samples have a higher sorption capacity towards carbon dioxide than for methane. The final pressures for the individual samples are shown in Figure 4a, and are 6 bar for P1 under a CO₂ atmosphere, 8.4 bar for a P1 CH₄ atmosphere, 8.76 bar for a P2 CO₂ atmosphere, and 10.12 bar for a P2 CH₄ atmosphere. For both samples, there was an observable drop in pressure inside the measuring ampoule, which indicates the occurrence of sorption phenomena in both methane and carbon dioxide atmospheres. Due to the specific shape of the samples, i.e., cuboid blocks, the measurements are very time-consuming. The use of samples of this shape also causes the equilibrium state to be reached much later than for samples in the form of powders. Observing the literature data [26,35], it can be observed that it takes a considerable amount of time to reach equilibrium, so experiments in this form must be staggered. As shown in Figure 4a,b, in the initial phase of the experiment, the adsorption increases rapidly before the sorption equilibrium is reached. This is evidenced by the fact that after about 20 h of measurements, there is little change in sorption.

The sorption capacity of P1 towards carbon dioxide was about 0.93 mmol/g, while for methane, the adsorbed amount was close to 0.68 mmol/g. The diameter of the particles has a significant effect on the value of adsorption on hard coal. CO₂, having a smaller diameter, can better penetrate the small diameter pores present in the coal material (see Table 2). Another parameter that can influence the adsorption value is the critical temperature of the sorbate and thus the state in which the particles are found. For carbon dioxide, the critical temperature is 304 K, so in the first stage of the experiment, under isothermal conditions, it exists in the form of vapour [36]. For methane, the critical temperature is 191 K, so it always appears as a gas during the experiments. Due to the occurrence of this phenomenon at the investigated temperature of 298 K, it is possible that a part of the pores is inaccessible to methane but is preferentially occupied by carbon dioxide particles thanks to the lower energy required to expand the pores. A similar phenomenon is also observed for P2. The

maximum sorption for carbon dioxide is about 0.5 mmol/g, and for methane it is about 0.33 mmol/g.

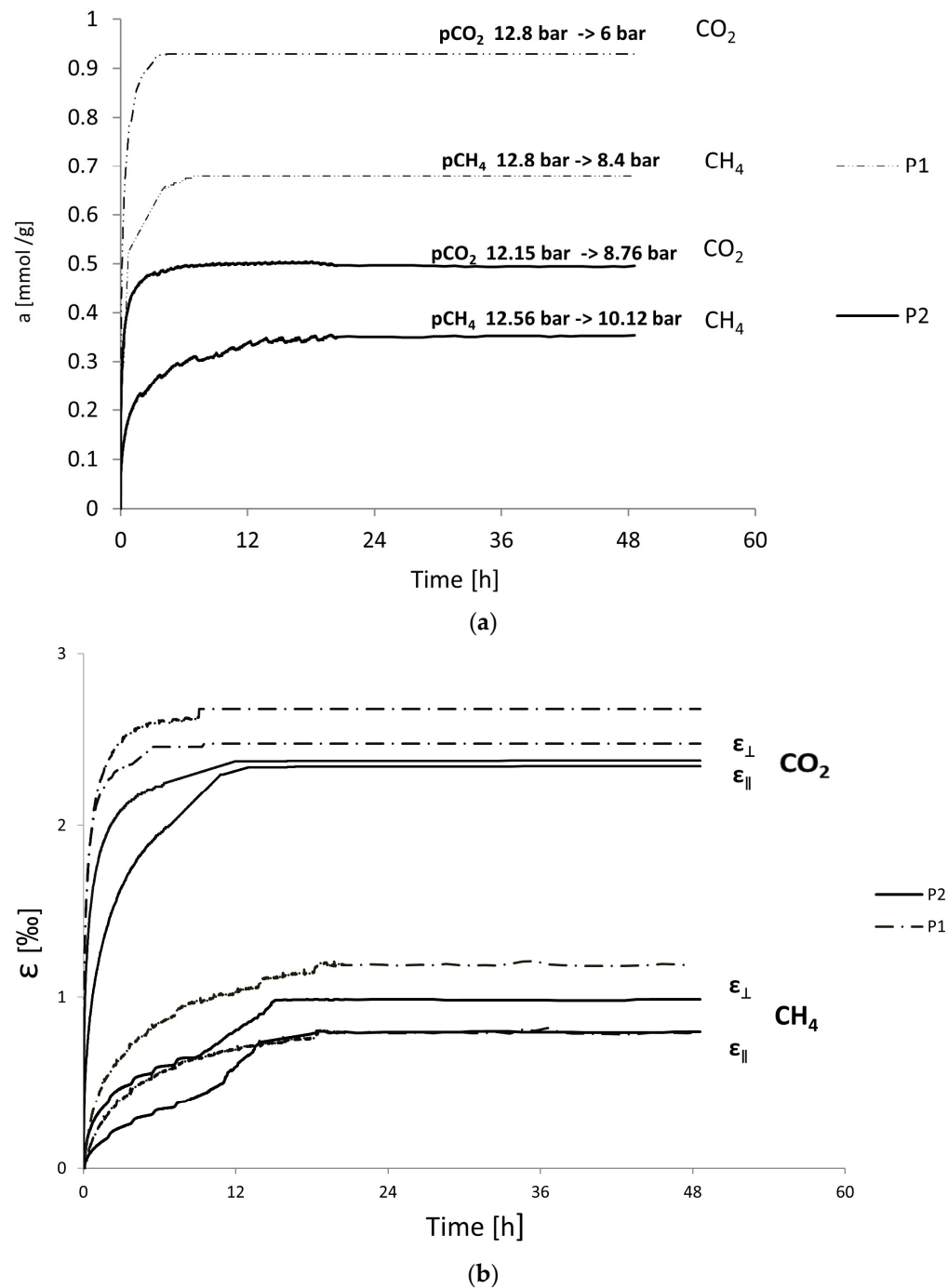


Figure 4. (a) Kinetics of CO₂ and CH₄ sorption. (b) Linear strains at 298 K for sample P1 and sample P2.

Table 2. Specification of the tested sorbates.

Sorbate	Melting Point (K)	Boiling Point (K)	Density at 1 atm, 273 K (kg/m ³)	Hybridization (-)	Kinetic Diameter (Å)
CO ₂	84.24	194.7 (sublimes)	1.977	sp	3.3
CH ₄	90.694	111.6	0.717	sp ³	3.8

A course of the change in linear expansion is shown in Figure 4b. Based on other researchers' observations [26,37], significant differences can also be observed in the behaviour of the coal matrix in dioxide and methane atmospheres. In Figure 4b, there is a clear difference in the strain values in the perpendicular and parallel directions. For P1, the differences in strain are much more pronounced than for P2 for both carbon dioxide and methane atmospheres. To convert values from linear expansion to volumetric expansion, the following formula (1) was used:

$$\varepsilon_v = 2\varepsilon_{\parallel} + \varepsilon_{\perp} \quad (1)$$

ε_v —volumetric strain

ε_{\parallel} —deformations parallel to the layering

ε_{\perp} —deformations perpendicular to the layering

For both samples, carbon dioxide sorption involving volumetric expansion was observably higher. For P1, the maximum volumetric strain was nearly 7.5% for CO₂, and nearly 4% for methane. For P2, the volumetric strain for carbon dioxide was 5%, while the strain for methane was close to 2%. The relationship between the amount of sorbed CO₂ and CH₄ and the sorption-induced swelling is presented in Figure 4a,b.

The results presented in Figure 4b show a relatively fast expansion of the coal matrix in the presence of carbon dioxide, and after 12 h, no more changes were observed for both samples. For the CH₄–coal system, it took about 20 h to reach an equilibrium state.

The data shown in Figure 4a are similar to those available in the literature and similarly describe the behaviour of the coal matrix. Research conducted by scientists has shown that hard coals have a higher affinity for the sorption of carbon dioxide than methane [26,35,38]. These values, however, may vary depending on the petrographic composition. Vitrinite is a maceral characterised by higher porosity than inertinite, which means that it can sorb a higher amount of vapour and gases within its structure [39]. P1, which has a higher vitrinite content, generally has a higher sorption capacity than P2. This was observed in the whole range of pressures and temperatures investigated. The sorption–dilatation properties of coal are also affected by such parameters.

Due to the correlation between the coal-swelling process and the amount of sorbed vapours and gases, these parameters should not be considered separately. When analysing the sorption kinetics graphs for P1, it can be observed that a state close to the sorption equilibrium is reached after about 12 h of measurement and the sample reaches a saturated state with both methane and carbon dioxide. Compared with another study [26], this was relatively fast. In that case, it took as long as 50 h to reach equilibrium. In addition, note the relationship between the expansion of coal and its sorption capacity shown in Figure 4a,b. For P1, the course of change over the time range studied was nearly linear for carbon dioxide sorption and nonlinear for methane sorption. The linear course of these changes was also shown in another publication [40]. In the pressure range similar to the tests presented in this publication, the course was the same. However, differences started to appear at higher pressures. From the data obtained, it can be concluded that the expansion kinetics is slower than the sorption kinetics compared to the situation if the phenomena had occurred evenly.

By analysing the data in Figure 4b, it is possible to compare them with the data available in the literature [35]. The hard coal in these studies differed in elemental composition from the coal presented in this article. Therefore, it is not possible to compare these results directly with each other. Maximum deformations were reached in the first 24 h from the start of the measurements in both methane and carbon dioxide atmospheres. As in this paper, deformations induced by the influence of carbon dioxide were several times higher than deformations induced by the presence of methane. For P1, it is less than 2 times more, for P2 about 2.5×, more while in Majewska's study [35], it was 3× more. The difference between Ceglarska-Stefańska's study and the study presented in this article was the behaviour of the sample after the maximum expansion was reached [41]. In our case, the sample, after being saturated with the tested gases, did not change its shape until the end

of the measurements. Similar behaviour was observed in another paper [28], where the petrographic composition was similar to that presented in this work. In Ceglarska-Stefańska's experiments, after reaching the maximum expansion, the sample slowly contracted. In our study, the relaxation phenomenon did not occur. Similar studies on sub-bituminous coals with vitrinite reflectance equal to 0.57% were carried out by Espinoza [29]. The main difference between the two experiments was the shape of the coal samples tested. In our case, they were cuboidal blocks, while Espinoza used cylindrical blocks of hard coal. In his case, higher expansion values were obtained for axial deformation, i.e., 0.006, while lower values were obtained for radial deformations, i.e., 0.004. These values are without a unit and are the result of the formulas proposed by the author.

An important parameter affecting sorption processes on hard coal is temperature, the effect of which on sorption–dilatometric properties is very evident under non-isothermal conditions. As is well known, the kinetic energy of sorbate molecules increases with increasing temperature. As the adsorption process is exothermic, an increase in temperature during the process can decrease the sorption capacity, which corresponds to the behaviour of P1 in a carbon dioxide atmosphere. As can be clearly seen in Figure 5a,b, P1 and P2 hardly increase their sorption capacity. The exception is P1, where a clear decrease in sorption capacity towards carbon dioxide is observed. A similar phenomenon can be found in the literature [26], in which researchers tested a wider range of temperatures and pressures, and both methane and carbon dioxide sorbed on the coal surface. These scientists identified the oxygen content as one of the reasons for this behaviour of the carbon material, which affects the number of active centres in the carbon matrix. An important parameter allowing discussion of the results is the diffusion coefficient, which can describe the decrease or increase in the sorption capacity in terms of temperature. With increasing temperature, the effective diffusion coefficient increases for methane [42,43]. Higher values of this parameter can be obtained for coals low in vitrinite, which may indicate differences in sorption capacity for P1 and P2 in the context of carbon dioxide. Figure 6a,b has been prepared based on the expansion kinetics and the sorption capacity of samples under non-isothermal conditions.

It was observed (Figure 7) that for the P1 sample and the carbon dioxide test, the sorption kinetics was slower than the expansion kinetics, because for a relatively small decrease in the sorption capacity, there was a clear change in the volumetric dimensions of the sample. In other cases, the change in sorption capacity due to a change in the volume dimensions of the sample was not so spectacular. As the temperature increases, samples treated with carbon dioxide undergo contraction. A completely opposite property was observable when the sample was tested in a methane atmosphere. Both P1 and P2 swelled with increasing temperature. Similar results were reported in another paper [44]. The purpose of this study was to investigate the behaviour of cuboidal coal samples under varying temperature conditions. In the case of dilatometric kinetics both for a vacuum and for helium, the changes in linear dimensions had exactly the same values, so when analysing the results of coal expansion, the thermal expansion parameter should be taken into account.

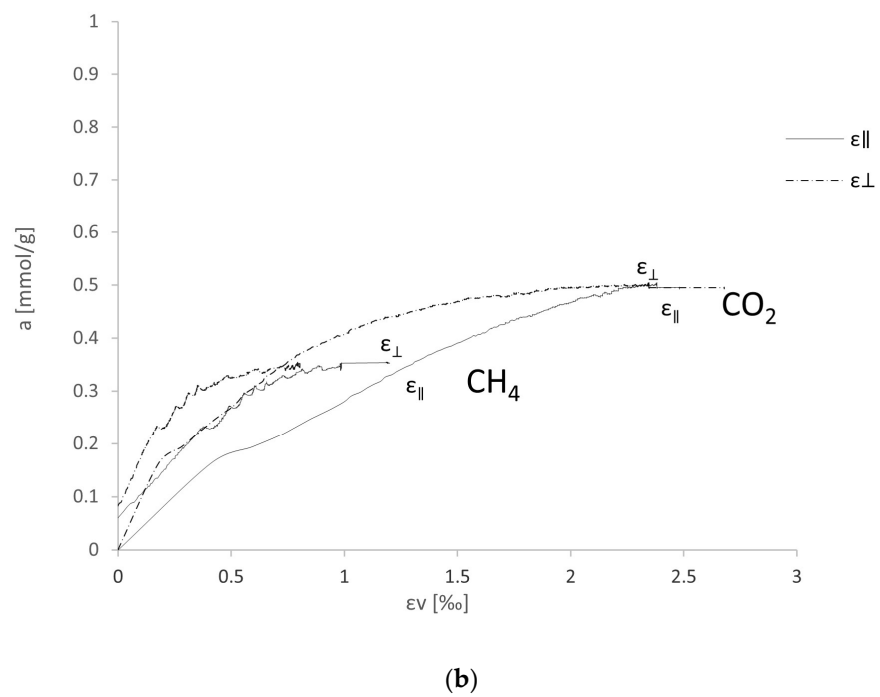
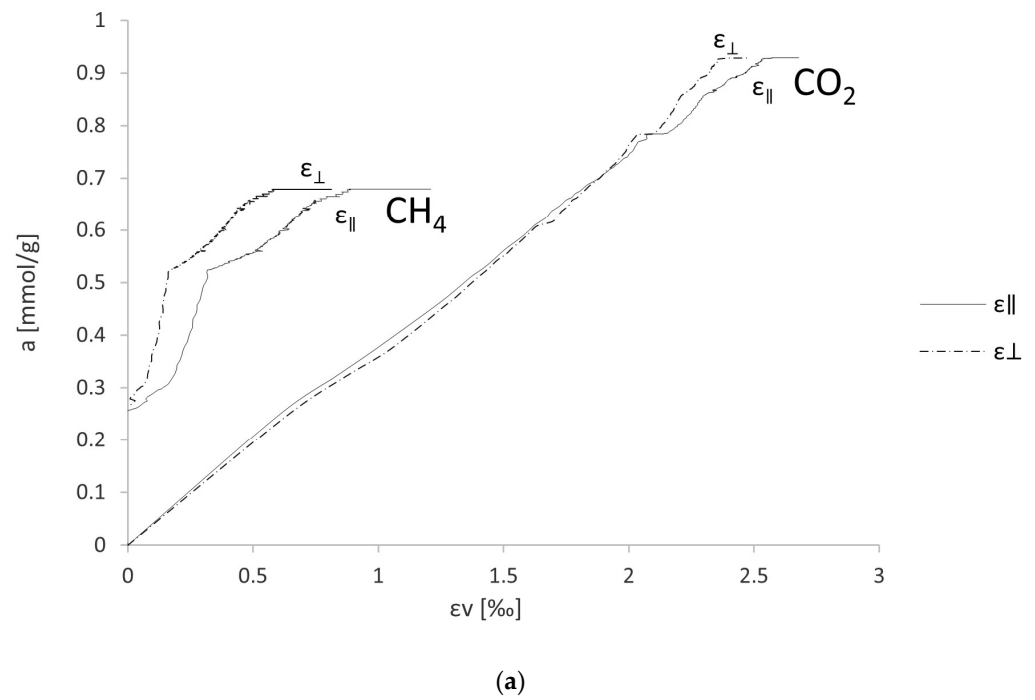
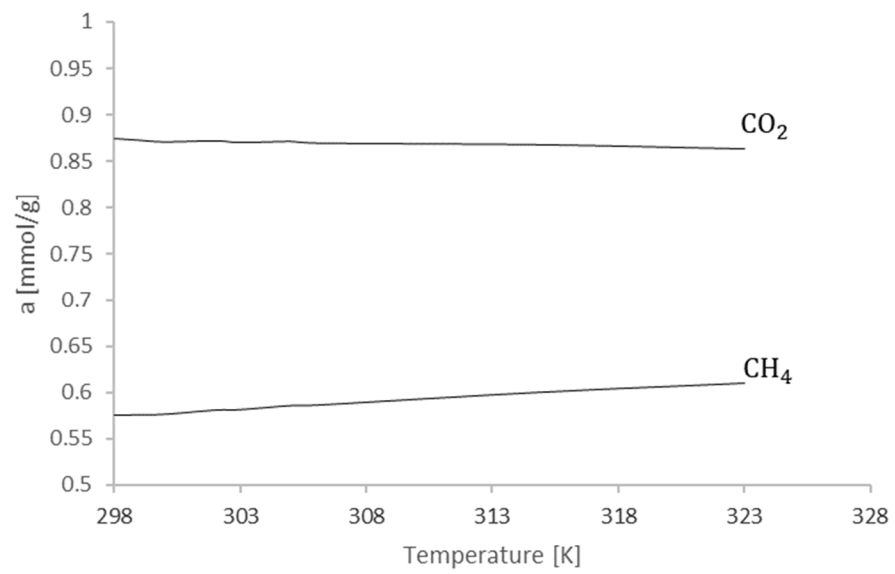
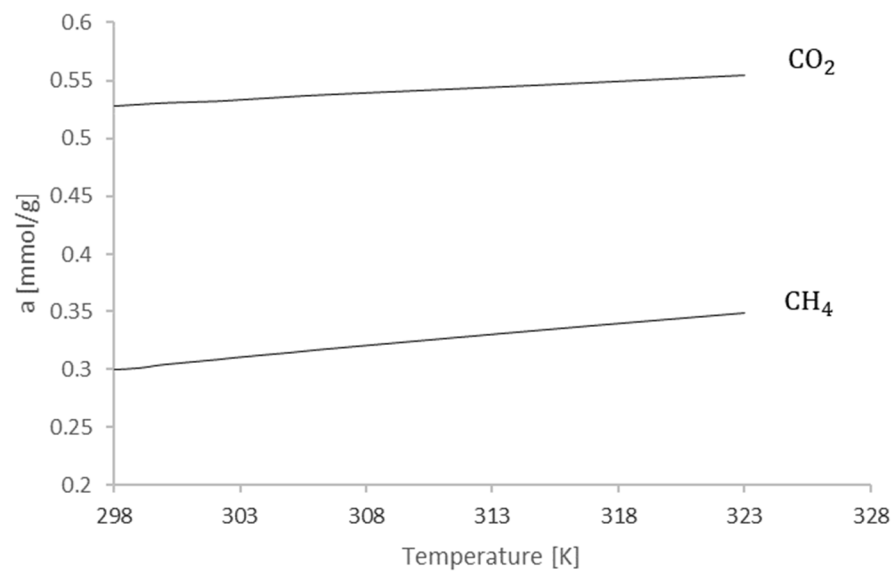


Figure 5. (a) Relationship between the amount of sorbed vapours and gases and the volumetric strain for sample P1. (b) Relationship between the amount of sorbed vapours and gases and the volumetric strain for sample P2.



(a)



(b)

Figure 6. (a) Change in sorption capacity for CO₂ and CH₄ depending on the temperature for P1. (b) Change in sorption capacity for CO₂ and CH₄ depending on the temperature for P2.

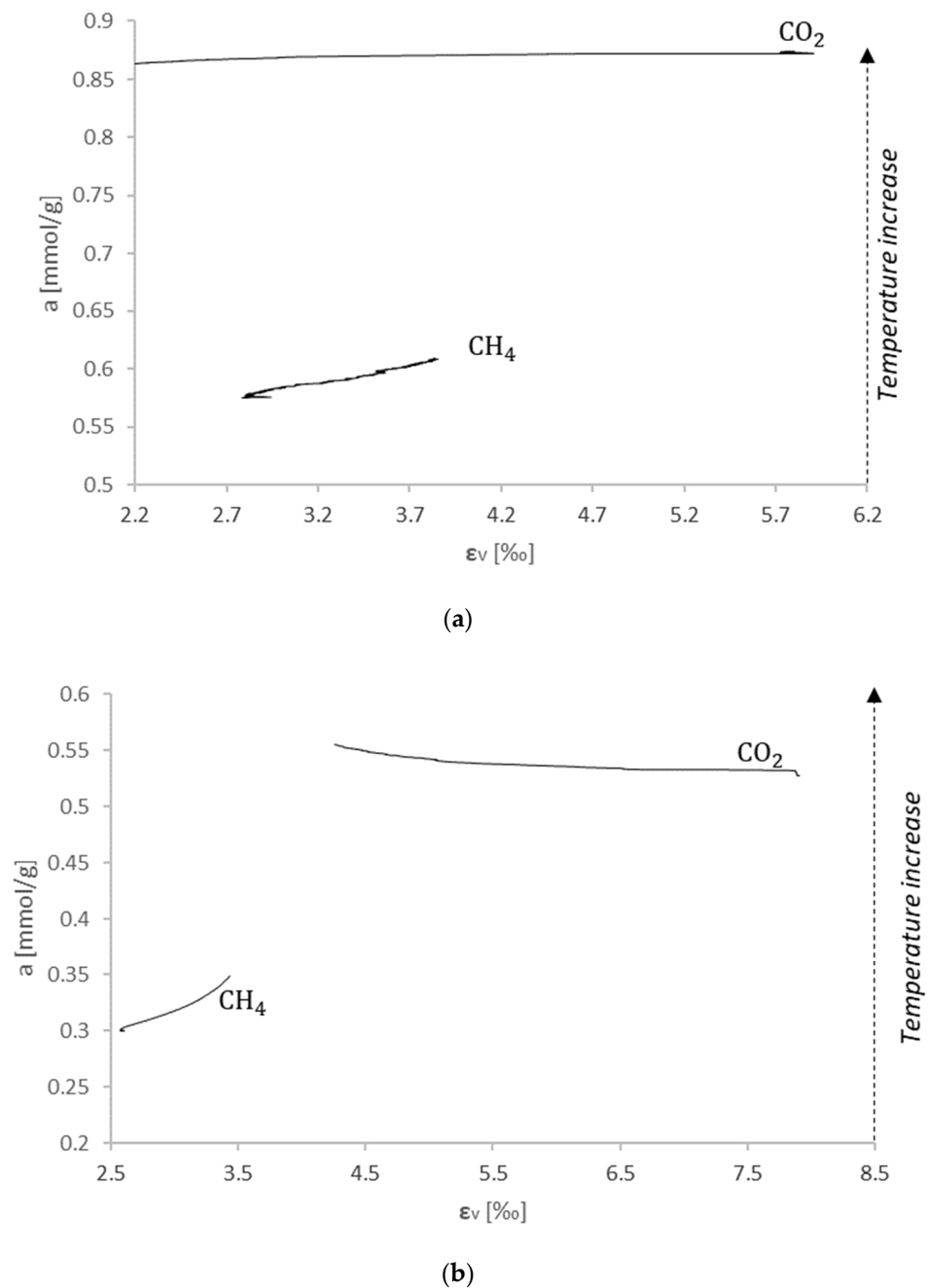


Figure 7. (a) Relationship between the amount of sorbed vapours and gases and the volumetric strain for sample P1 under non-isothermic conditions. (b) Relationship between the amount of sorbed vapours and gases and the volumetric strain for sample P2 under non-isothermic conditions.

5. Conclusions

- Change in the linear dimensions of the sample in the isothermal process due to carbon dioxide sorption is $2.5\times$ greater than for methane sorption, with a noticeable difference between the two samples due to the different vitrinite content.
- The relationship between sorption capacity and volumetric expansion in the isothermal process for carbon dioxide for P1 is nearly linear, while for methane it is increasing. For P2, the graph has a curved shape. In the analysis of the later phase of the experiment, the rate of increase in volumetric strain is higher than the rate of increase in sorption capacity.

- Investigations carried out with increasing temperatures provided new data on the behaviour of the coal matrix. As the temperature increased, a slight increase in the sorption capacity of the sample was observed, with the sample shrinking in a carbon dioxide atmosphere and expanding in a methane atmosphere.
- The analysis of sorption capacity changes as a function of volume expansion under non-isothermal conditions provides relevant information about the carbon–gas system. As the temperature increases, no significant change in sorption capacity is observed, while a change in the volume dimensions of the sample is observed, indicating that the parameter related to the movement of vapours and gases within the carbon matrix has a greater influence on this process.

Author Contributions: Conceptualization, P.B.; methodology, P.B. and K.Z.; validation, P.B. and K.C.; formal analysis, P.B., S.K., K.C., A.S. and K.Z.; investigation, S.K.; resources, P.B. and K.Z.; data curation, S.K.; writing—original draft preparation, S.K. and K.C.; writing—review and editing, P.B. and K.Z.; visualization, S.K.; supervision, P.B.; project administration, K.Z.; funding acquisition, K.Z. All authors have read and agreed to the published version of the manuscript.

Funding: The authors gratefully acknowledge financial support from the “Initiative of Excellence—Research University—IDUB” program of AGH University of Science and Technology in Krakow, Poland.

Institutional Review Board Statement: Not applicable.

Informed Consent Statement: Not applicable.

Conflicts of Interest: The authors declare no conflict of interest.

References

1. International Energy Agency. *Coal 2019; Market Report Series: Coal*; OECD: Paris, France, 2019; ISBN 9789264391604.
2. Kowalska, N.; Brodawka, E.; Smoliński, A.; Zarebska, K. The European Education Initiative as a Mitigation Mechanism for Energy Transition. *Energies* **2022**, *15*, 6633. [[CrossRef](#)]
3. Kelemen, P.; Benson, S.M.; Pilorgé, H.; Psarras, P.; Wilcox, J. An Overview of the Status and Challenges of CO₂ Storage in Minerals and Geological Formations. *Front. Clim.* **2019**, *1*, 9. [[CrossRef](#)]
4. Hassanpouryouzband, A.; Yang, J.; Tohidi, B.; Chuvilin, E.; Istomin, V.; Bukhanov, B.; Cheremisin, A. CO₂ Capture by Injection of Flue Gas or CO₂-N₂ Mixtures into Hydrate Reservoirs: Dependence of CO₂ Capture Efficiency on Gas Hydrate Reservoir Conditions. *Environ. Sci. Technol.* **2018**, *52*, 4324–4330. [[CrossRef](#)] [[PubMed](#)]
5. Hassanpouryouzband, A.; Joonaki, E.; Edlmann, K.; Haszeldine, R.S. Offshore Geological Storage of Hydrogen: Is This Our Best Option to Achieve Net-Zero? *ACS Energy Lett.* **2021**, *6*, 2181–2186. [[CrossRef](#)]
6. Markewitz, P.; Kuckshinrichs, W.; Leitner, W.; Linssen, J.; Zapp, P.; Bongartz, R.; Schreiber, A.; Müller, T.E. Worldwide Innovations in the Development of Carbon Capture Technologies and the Utilization of CO₂. *Energy Environ. Sci.* **2012**, *5*, 7281–7305. [[CrossRef](#)]
7. Zhang, D.; Song, J. Mechanisms for Geological Carbon Sequestration. *Procedia IUTAM* **2014**, *10*, 319–327. [[CrossRef](#)]
8. Page, B.; Stern, N.; Hameister Oam, J. *Global Status of CCS 2020*; Global CCS Institute: Melbourne, Australia, 2020.
9. Karacan, C.Ö.; Ruiz, F.A.; Cotè, M.; Phipps, S. Coal Mine Methane: A Review of Capture and Utilization Practices with Benefits to Mining Safety and to Greenhouse Gas Reduction. *Int. J. Coal Geol.* **2011**, *86*, 121–156. [[CrossRef](#)]
10. Mangi, H.N.; Detian, Y.; Hameed, N.; Ashraf, U.; Rajper, R.H. Pore Structure Characteristics and Fractal Dimension Analysis of Low Rank Coal in the Lower Indus Basin, SE Pakistan. *J. Nat. Gas Sci. Eng.* **2020**, *77*, 103231. [[CrossRef](#)]
11. Moore, T.A. Coalbed Methane: A Review. *Int. J. Coal Geol.* **2012**, *101*, 36–81. [[CrossRef](#)]
12. Gürdal, G.; Yalçın, M.N. Gas Adsorption Capacity of Carboniferous Coals in the Zonguldak Basin (NW Turkey) and Its Controlling Factors. *Fuel* **2000**, *79*, 1913–1924. [[CrossRef](#)]
13. Corrente, N.J.; Zarebska, K.; Neimark, A. V Deformation of Nanoporous Materials in the Process of Binary Adsorption: Methane Displacement by Carbon Dioxide from Coal. *J. Phys. Chem. C* **2021**, *125*, 21310–21316. [[CrossRef](#)]
14. Guo, D.; Guo, X. The Influence Factors for Gas Adsorption with Different Ranks of Coals. *Adsorpt. Sci. Technol.* **2017**, *36*, 904–918. [[CrossRef](#)]
15. Zarebska, K.; Baran, P.; Cygankiewicz, J.; Dudzińska, A.; Zarebska, K.; Baran, P.; Cygankiewicz, J.; Dudzińska, A. Sorption of Carbon Dioxide on Polish Coals in Low and Elevated Pressure. *Fresenius Environ. Bull.* **2012**, *21*, 4003–4008.
16. Macuda, J.; Baran, P.; Wagner, M. Evaluation of the Presence of Methane in Złoczew Lignite: Comparison with Other Lignite Deposits in Poland. *Nat. Resour. Res.* **2020**, *29*, 3841–3856. [[CrossRef](#)]
17. Jian, X.; Guan, P.; Zhang, W. Carbon Dioxide Sorption and Diffusion in Coals: Experimental Investigation and Modeling. *Sci. China Earth Sci.* **2012**, *55*, 633–643. [[CrossRef](#)]
18. Hildenbrand, A.; Krooss, B.M.; Busch, A.; Gaschnitz, R. Evolution of Methane Sorption Capacity of Coal Seams as a Function of Burial History—A Case Study from the Campine Basin, NE Belgium. *Int. J. Coal Geol.* **2006**, *66*, 179–203. [[CrossRef](#)]

19. Wojtacha-Rychter, K.; Howaniec, N.; Smoliński, A. Effect of Porous Structure of Coal on Propylene Adsorption from Gas Mixtures. *Sci. Rep.* **2020**, *10*, 11277. [[CrossRef](#)]
20. Clarkson, C.R.; Marc Bustin, R. Variation in Micropore Capacity and Size Distribution with Composition in Bituminous Coal of the Western Canadian Sedimentary Basin: Implications for Coalbed Methane Potential. *Fuel* **1996**, *75*, 1483–1498. [[CrossRef](#)]
21. Laxminarayana, C.; Crosdale, P.J. Role of Coal Type and Rank on Methane Sorption Characteristics of Bowen Basin, Australia Coals. *Int. J. Coal Geol.* **1999**, *40*, 309–325. [[CrossRef](#)]
22. Sadasivam, S.; Masum, S.; Chen, M.; Stańczyk, K.; Thomas, H. Kinetics of Gas Phase CO₂ Adsorption on Bituminous Coal from a Shallow Coal Seam. *Energy Fuels* **2022**, *36*, 8360–8370. [[CrossRef](#)]
23. Zhang, W.; Jiang, S.; Wang, K.; Wang, L.; Xu, Y.; Wu, Z.; Shao, H.; Wang, Y.; Miao, M. Thermogravimetric Dynamics and FTIR Analysis on Oxidation Properties of Low-Rank Coal at Low and Moderate Temperatures. *Int. J. Coal Prep. Util.* **2015**, *35*, 39–50. [[CrossRef](#)]
24. Talapatra, A. A Study on the Carbon Dioxide Injection into Coal Seam Aiming at Enhancing Coal Bed Methane (ECBM) Recovery. *J. Pet. Explor. Prod. Technol.* **2020**, *10*, 1965–1981. [[CrossRef](#)]
25. Talapatra, A.; Karim, M.M. The Influence of Moisture Content on Coal Deformation and Coal Permeability during Coalbed Methane (CBM) Production in Wet Reservoirs. *J. Pet. Explor. Prod. Technol.* **2020**, *10*, 1907–1920. [[CrossRef](#)]
26. Czerw, K.; Baran, P.; Zarebska, K. Application of the Stretched Exponential Equation to Sorption of Mine Gases and Sorption Induced Swelling of Bituminous Coal. *Int. J. Coal Geol.* **2017**, *173*, 76–83. [[CrossRef](#)]
27. Ranathunga, A.S.; Perera, M.S.A.; Ranjith, P.G.; Rathnaweera, T.D.; Zhang, X.G. Effect of Coal Rank on CO₂ Adsorption Induced Coal Matrix Swelling with Different CO₂ Properties and Reservoir Depths. *Energy Fuels* **2017**, *31*, 5297–5305. [[CrossRef](#)]
28. Czerw, K. Methane and Carbon Dioxide Sorption/Desorption on Bituminous Coal—Experiments on Cubicoid Sample Cut from the Primal Coal Lump. *Int. J. Coal Geol.* **2011**, *85*, 72–77. [[CrossRef](#)]
29. Espinoza, D.N.; Vandamme, M.; Pereira, J.M.; Dangla, P.; Vidal-Gilbert, S. Measurement and Modeling of Adsorptive-Poromechanical Properties of Bituminous Coal Cores Exposed to CO₂: Adsorption, Swelling Strains, Swelling Stresses and Impact on Fracture Permeability. *Int. J. Coal Geol.* **2014**, *134*, 80–95. [[CrossRef](#)]
30. Gaowei, Y.; Chunlin, Z.; Liupeng, H.; Xinjun, Z. Measurement and Modeling of Temperature Evolution during Methane Desorption in Coal. *Sci. Rep.* **2020**, *10*, 3146. [[CrossRef](#)]
31. Wang, Z.; Tang, X.; Yue, G.; Kang, B.; Xie, C.; Li, X. Physical Simulation of Temperature Influence on Methane Sorption and Kinetics in Coal: Benefits of Temperature under 273.15 K. *Fuel* **2015**, *158*, 207–216. [[CrossRef](#)]
32. Jakubów, A.; Tor, A.; Tobczyk, S. Wyrzut Metanu i Skał w Drażonej Lunecie Rurowej Do Szybu II Na Poziomie 1000m w KRK Pniówek- Okoliczności, Przyczyny i Skutki. In Proceedings of the Szkoła Eksploatacji Podziemnej, Szczyrk, Poland, 7–21 February 2003.
33. *Ocena Stanu Bezpieczeństwa Pracy, Ratownictwa Górniczego Oraz Bezpieczeństwa Powszechnego w Związku z Działalnością Górniczo-Geologiczną w 2015r*; WUG: Katowice, Poland, 2016.
34. Wasilewski, S.; Jamróz, P. Wybrane Katastrofy i Wypadki w Górnictwie Polskim—Zebranie Danych. *Pr. Inst. Mech. Górotworu PAN* **2018**, *20*, 197–206.
35. Majewska, Z.; Ceglarska-Stefańska, G.; Majewski, S.; Ziętek, J. Binary Gas Sorption/Desorption Experiments on a Bituminous Coal: Simultaneous Measurements on Sorption Kinetics, Volumetric Strain and Acoustic Emission. *Int. J. Coal Geol.* **2009**, *77*, 90–102. [[CrossRef](#)]
36. Zarebska, K.; Ceglarska-Stefańska, G. The Change in Effective Stress Associated with Swelling during Carbon Dioxide Sequestration on Natural Gas Recovery. *Int. J. Coal Geol.* **2008**, *74*, 167–174. [[CrossRef](#)]
37. Li, J.; Li, B.; Cheng, Q.; Gao, Z. Characterization of Anisotropic Coal Permeability with the Effect of Sorption-Induced Deformation and Stress. *Fuel* **2022**, *309*, 122089. [[CrossRef](#)]
38. Nikoosokhan, S.; Vandamme, M.; Dangla, P. A Poromechanical Model for Coal Seams Saturated with Binary Mixtures of CH₄ and CO₂. *J. Mech. Phys. Solids* **2014**, *71*, 97–111. [[CrossRef](#)]
39. Guo, P. A Theoretical Model for Coal Swelling Induced by Gas Adsorption in the Full Pressure Range. *Adsorpt. Sci. Technol.* **2020**, *38*, 94–112. [[CrossRef](#)]
40. Ceglarska-Stefańska, G.; Zarebska, K. Expansion and Contraction of Variable Rank Coals During the Exchange Sorption of CO₂ and CH₄. *Adsorpt. Sci. Technol.* **2002**, *20*, 49–62. [[CrossRef](#)]
41. Ceglarska-Stefańska, G.; Zarebska, K. The Competitive Sorption of CO₂ and CH₄ with Regard to the Release of Methane from Coal. *Fuel Process. Technol.* **2002**, *77–78*, 423–429. [[CrossRef](#)]
42. Wierzbicki, M. Changes in the Sorption/Diffusion Kinetics of a Coal-Methane System Caused by Different Temperatures and Pressures. *Gospod. Surowcami Miner.—Miner. Resour. Manag.* **2013**, *29*, 155–168. [[CrossRef](#)]
43. Dutka, B.; Kudasik, M.; Pokryszka, Z.; Skoczylas, N.; Topolnicki, J.; Wierzbicki, M. Balance of CO₂/CH₄ Exchange Sorption in a Coal Briquette. *Fuel Process. Technol.* **2013**, *106*, 95–101. [[CrossRef](#)]
44. Baran, P.; Czerw, K.; Samojeden, B.; Czuma, N.; Zarebska, K.; Baran, P.; Czerw, K.; Samojeden, B.; Czuma, N.; Zarebska, K. The Influence of Temperature on the Expansion of a Hard Coal-Gas System. *Energies* **2018**, *11*, 2735. [[CrossRef](#)]

Disclaimer/Publisher’s Note: The statements, opinions and data contained in all publications are solely those of the individual author(s) and contributor(s) and not of MDPI and/or the editor(s). MDPI and/or the editor(s) disclaim responsibility for any injury to people or property resulting from any ideas, methods, instructions or products referred to in the content.